ALD-METAL UNCOOLED BOLOMETER

S. Yoneoka[1], M. Liger[2], G. Yama[2], R. Schuster[2], F. Purkl[2], J Provine[1], F. B. Prinz[1], R. T. Howe[1], and T. W. Kenny[1]
[1]Stanford University, Stanford, California, USA
[2]Robert Bosch LLC Research and Technology Center, Palo Alto, California, USA

ABSTRACT

This paper presents an uncooled infrared bolometer using a metal thin film that is formed by atomic layer deposition (ALD). Nanometer-thick freestanding layers enabled by ALD have the potential to improve the performance of bolometers with achieving low thermal conductance and near optimal optical properties. The fabrication and characterization of the first implementation are described as well as the electrical properties of ALD platinum films.

INTRODUCTION

Infrared detectors in the long-wavelength infrared (LWIR) region (8-14 μm) are classified as photon detectors and thermal detectors [1]. Photon detectors measure free electrons or holes generated by an incoming radiation. Thermal detectors measure the temperature change produced by an absorbed radiation with various transduction mechanisms including electrical resistance change, pyroelectricity, thermoelectricity, and thermal expansion [1-4]. Although photon detectors can achieve superior performance, thermal detectors are more suitable for low-cost applications since photon detectors generally require cooling to cryogenic temperature [1, 5]. Specifically, thermal detectors with temperature dependent resistors, which are called bolometers, are widely used for uncooled infrared focal plane arrays.

A standard bolometer consists of a thermally isolated freestanding membrane, supporting beams, and a thermistor (Fig. 1). The absorption of incoming infrared radiation in the membrane increases the temperature of the thermistor. One of the most important figures of merits of bolometers is noise-equivalent temperature difference (NETD) [1]. NETD is expressed as

$$NETD = \frac{G_{th} v_n}{\alpha \eta I_b R_0 \frac{d\Phi}{dT}} \qquad (1)$$

where G_{th} is total thermal conductance between the absorber membrane and the sensor substrate, v_n is total noise of the bolometer, α is temperature coefficient of resistance (TCR), η is absorption coefficient, I_b is bias current, R_0 is electrical resistance of the thermistor, and $d\Phi/dT$ is the change of the incident radiant flux in the 8-14 μm band per temperature change on the radiant source. The total noise is the root mean square of Johnson noise, 1/f noise, temperature fluctuation noise, and photon noise. The improvement of the bolometers' performance can be achieved by minimizing the thermal conductance of the suspended structure, maximizing the absorption coefficient, and maximizing the ratio of the TCR to the normalized 1/f noise [1, 6].

Conventional micromachined bolometers consist of multiple functional layers to optimize their performance. Vanadium oxide, α-Si, poly-SiGe, and metal are commonly used as thermistor [1, 7-9]. Silicon dioxide and silicon nitride are often used as the supporting and absorbing layers because of their small thermal conductivity. For the infrared absorption, most bolometers rely on an optical cavity with an impedance-matched film [10, 11]. These functional layers can be replaced by one metal layer to further reduce the thermal conductance and simplify the fabrication process. However, this requires a film thickness in the order of nanometers since the impedance of the film must approach that of free space in order to absorb the wavelengths of the interest [12].

In this paper, we propose an uncooled infrared bolometer using a few-nanometer-thick platinum (Pt) film that is formed by atomic layer deposition (ALD). ALD is used to reliably deposit Pt films with less than 10-nm thickness. While Pt has a relatively low TCR it also has low 1/f noise, good linearity, and low hysteresis, making it a good temperature sensing material overall. The ALD Pt film is used both as the absorber and as supporting beams. The thermal capacitance is greatly reduced since the membrane is much thinner than the conventional dielectric absorbers. Therefore, the thermal insulation can be further improved while keeping the thermal time constant at an acceptable value.

DESIGN

The schematic of the proposed bolometer is shown in Fig. 1. The bolometer consists of a 50 × 50-μm freestanding infrared absorber and two supporting beams with 50-μm length and 3-μm width. The U-shaped trenches with 1-μm

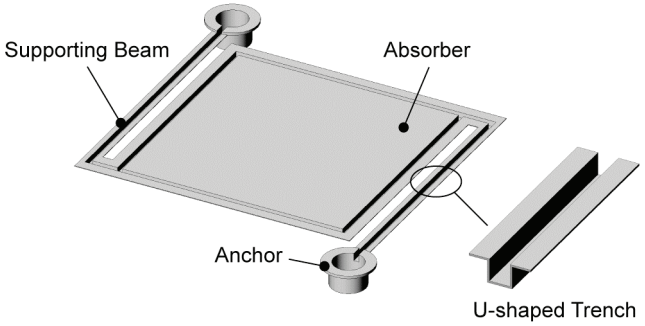

Figure 1: Schematic of the proposed bolometer.

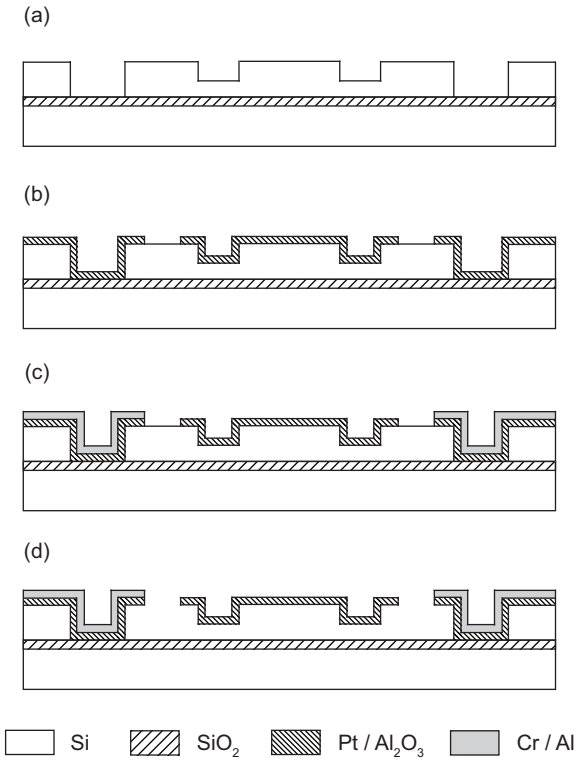

Figure 2: Cross-sectional images of the fabrication process. (a) U-shaped trenches and holes are etched by DRIE and RIE, respectively. (b) The Al_2O_3 and Pt films are formed by ALD. Both layers are defined with ion milling. (c) The Cr and Al films are deposited and defined by wet etching. (d) The devices are released with XeF_2 vapor etching.

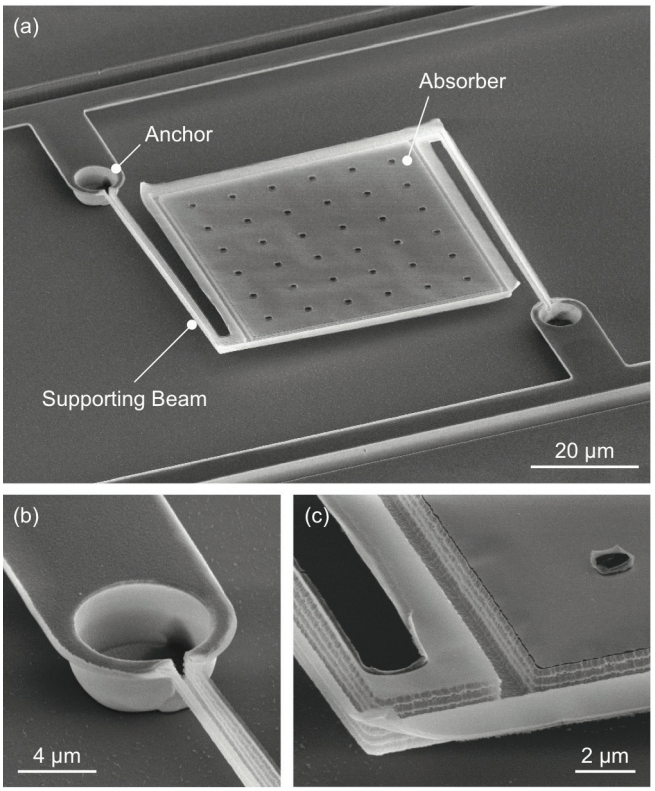

Figure 3: (a) SEM image of the fabricated bolometer tilted by 55 degrees. (b) Higher magnification of the anchor. (c) Higher magnification of the U-shaped trench.

depth are introduced on the periphery of the absorber and the center of the supporting beams to enhance the mechanical stiffness of the bolometer. Metal anchors are designed to support the bolometer with a minimal fill factor loss and to control the gap size of the optical cavity between the absorber and the bottom layer. This gap size is set to maximize the absorption coefficient of the bolometer. For metal films with a sheet resistance matching the impedance of free space, the optimal gap size to absorb LWIR is 2-3.5 μm depending on the mirror material.

FABRICATION PROCESS

The fabrication process of the devices starts from a silicon-on-insulator (SOI) wafer with a 3.3-μm device layer and 400-nm buried oxide layer (Fig. 2). In this process, the device layer is used as a sacrificial layer to form bolometer structures. At the first step, U-shaped trenches and holes for anchors are defined with deep reactive ion etching (DRIE) and reactive ion etching (RIE), respectively. While DRIE is used for the U-shaped trenches to obtain vertical albeit scalloped sidewalls, RIE is used for the holes to have slightly tapered sidewall to aid in conformal metal deposition during sputtering later in the process. The aluminum oxide (Al_2O_3) and Pt layers are then formed by ALD. Both layers uniformly coat the trenches and holes. The Al_2O_3 film is deposited using trimethylaluminum [TMA, $Al(CH_3)_3$] and H_2O as precursors, and the Pt film is deposited using (methylcyclopentadienyl)trimethylplatinum [$MeCpPtMe_3$, $(CH_3C_5H_4)Pt(CH_3)_3$] and oxygen [13, 14]. In this process, Al_2O_3 is used as a seeding layer for ALD Pt. Both ALD layers are etched with ion milling to define the bolometer structure. The 20-nm chromium (Cr) and 200-nm aluminum (Al) films are sputtered to form the metal anchors and bond pads, followed by metal etching with Cr and Al etchants. The Cr layer serves as adhesion layer and prevents the Al etchant from etching the Al_2O_3 layer [15]. Finally, the devices are released with XeF_2 vapor etching. The device layer under the bond pads is not attacked by XeF_2 vapor etching since it is sealed with Cr and Al layers.

Fig. 3 shows Scanning Electron Microscope (SEM) images of a fabricated device. A bolometer with 50 × 50-μm absorber is successfully fabricated using 7.0-nm Pt and 7.7-nm Al_2O_3 films. The aspect ratio of the freestanding structure is greater than 3000:1. The sidewalls of the U-shaped trenches increase the stiffness of the membrane along the out-of-plane direction, which maintains the flatness of the released structure. Fig. 3(b) and 3(c) show a higher magnification of the anchor and U-shaped trench. The typical DRIE scallops can be observed since the ALD films uniformly coat the sacrificial layer. The holes on the

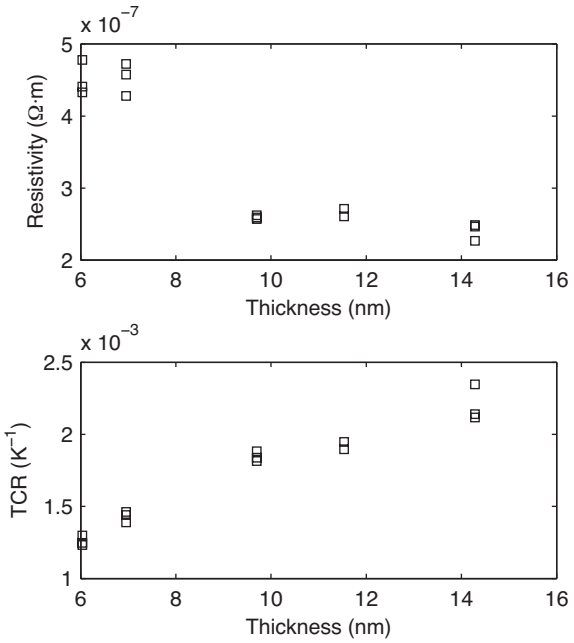

Figure 4: Electrical resistivity and TCR of ALD Pt films with different thicknesses. Multiple devices are measured at each thickness.

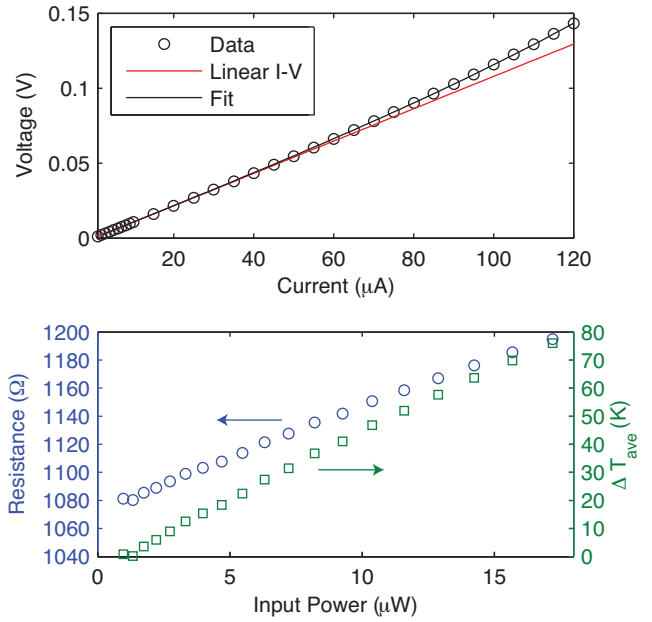

Figure 5: (a) I-V curve of the fabricated bolometer. (b) Electrical resistance and average temperature increase of the bolometer as a function of the input power.

absorber are designed to enhance the etching of the Si sacrificial layer.

EXPERIMENTAL RESULTS

The electrical resistivity and TCR of ALD Pt with different thicknesses are measured by a four-wire method at room temperature (Fig. 4). The thickness of Pt films is calibrated with the observations by a transmission electron microscopy. The measured electrical resistivity and TCR deviate form those of bulk Pt. The average electrical resistivity and TCR of 7.0-nm Pt are 4.5×10^{-7} Ω·m and 1.4×10^{-3} K^{-1}, respectively. Thinner films have larger electrical resistivity and smaller TCR since the film thicknesses are smaller than the electron mean free path of bulk Pt and the surface scattering becomes dominant with decreasing film thickness [16].

After the characterization of ALD Pt films, the I-V curve of the fabricated bolometer is measured at ~0.25 Pa (Fig. 5(a)). The I-V curve becomes nonlinear since the temperature of the bolometer increases with joule heating. Fig. 5(b) shows the electrical resistance and average temperature change of the bolometer as a function of the input power. The effective thermal conductance of the bolometer is 2.10×10^{-7} W/K based on the linear fitting of Fig. 5(b). Although the maximum temperature rise during I-V measurement is on the absorber, the electrical resistance of the supporting beams is dominant in the total resistance. Therefore, the measured thermal conductance is larger than the thermal conductance between the absorber and the substrate. The thermal time constant of the bolometer is

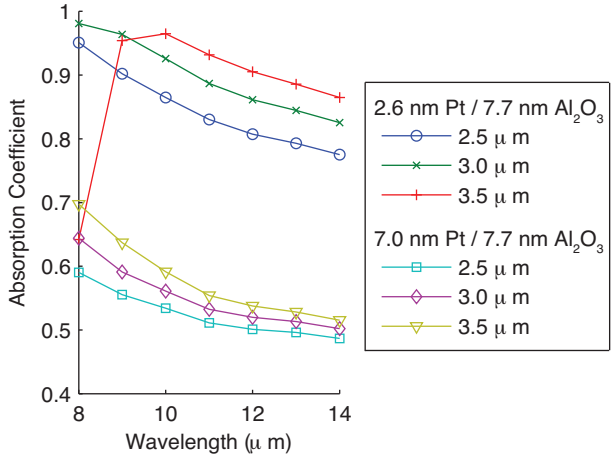

Figure 6: Estimated absorption coefficient of the bolometer with an optical cavity for two different film thicknesses. Different symbols show different gap sizes of the cavity. The refractive index of a 2.6-nm Pt film is assumed to be same with that of a 7.0-nm Pt film.

approximately 0.6 ms when the specific heat capacities of the Pt and Al_2O_3 films are same with the bulk properties. The absorption coefficient of the bolometer is calculated by applying the transfer matrix method with assuming that a metal reflective layer is implemented on the oxide layer (Fig. 6). The refractive indices of Pt and Al_2O_3 layers for this simulation are determined by IR ellipsometry. The absorption coefficient of the fabricated bolometer over the LWIR range is estimated to be 0.52-0.70 when a gap size of

the optical cavity is 3.5 μm (Fig. 6). The simulation results show the absorption coefficient can be improved with a 2.6-nm Pt film if the measured refractive index is size independent. The estimated noise-equivalent power referred to 1 Hz bandwidth of the bolometer is 5.17×10^{-12} W/√Hz with assuming 60% absorption efficiency, 200-μA bias current, and negligible 1/f noise [1]. The corresponding NETD is 184 mK when the F-number is 1 and the integration time is 150 μsec.

CONCLUSION

In this work, we fabricated and characterized uncooled infrared bolometers using ALD Pt films. The flat 50 × 50-μm freestanding membrane is successfully fabricated with nanometer-thick Pt and Al_2O_3 films, which demonstrates the feasibility of the proposed bolometers. Based on the experimental and simulation results, NETD of the fabricated device is estimated to be 184 mK assuming negligible 1/f noise. Future work includes 1/f noise characterization of ALD Pt films and the fabrication of bolometer arrays with reflectors.

ACKNOWLEDGEMENT

This work was performed under the Center on Interfacial Engineering for Microelectromechanical Systems, funded by DARPA grant HR0011-06-0049 and managed by Dr. D. L. Polla and Dr. A. I. Akinwande. Additional support was provided by the National Nanotechnology Infrastructure Network facilities funded by National Science Foundation.

REFERENCES

[1] P. W. Kruse and D. D. Skatrud, *Uncooled infrared imaging arrays and systems,* Academic Press, 1997.

[2] P. Muralt, "Micromachined infrared detectors based on pyroelectric thin films," *Rep. Prog. Phys.,* vol. 64, pp. 1339-1388, 2001.

[3] I. H. Choi and K. D. Wise, "A silicon-thermopile-based infrared sensing array for use in automated manufacturing," *IEEE Trans. Electron Devices,* vol. 33, pp. 72-79, 1986.

[4] T. W. Kenny, J. K. Reynolds, J. A. Podosek, E. C. Vote, L. M. Miller, H. K. Rockstad, and W. J. Kaiser, "Micromachined infrared sensors using tunneling displacement transducers," *Rev. Sci. Instrum.,* vol. 67, pp. 112-128, 1996.

[5] P. W. Kruse, "A comparison of the limits to the performance of thermal and photon detector imaging arrays," *Infrared Phys. Technol*., vol. 36, pp. 869-882, 1995.

[6] P. C. Shan, Z. Çelik-Butler, D. P. Butler, A. Jahanzeb, C. M. Travers, W. Kula, and R. Sobolewski, "Investigation of semiconducting YBaCuO thin films: a new room temperature bolometer," *J. Appl. Phys.,* vol. 80, pp. 7118-7123, 1996.

[7] F. Niklaus, C. Vieider, and H. Jakobsen, "MEMS-based uncooled infrared bolometer arrays – a review," in *Proc. SPIE,* 2007, vol. 6836, pp. 0D1-0D15.

[8] S. Sedky, P. Fiorini, K. Baert, L. Hermans, and R. Mertens, "Characterization and optimization of infrared poly SiGe bolometers," *IEEE Trans. Electron Devices*, vol. 46, pp. 675-682, 1999.

[9] A. Tanaka, S. Matsumoto, N. Tsukamoto, S. Itoh, K. Chiba, T. Endoh, A. Nakazato, K. Okuyama, Y. Kumazawa, M. Hijikawa, H. Gotoh, T. Tanaka, and N. Teranishi, "Infrared focal plane array incorporating silicon IC process compatible bolometer," *IEEE Trans. Electron Devices,* vol. 43, pp. 1844-1850, 1996.

[10] W. W. Salisbury, "Absorbent body for electromagnetic waves," U.S. Patent 2599944, 1952.

[11] P. A. Silberg, "Infrared absorption of three-layer films," *J. Opt. Soc. Am.,* vol. 47, pp. 575-578, 1957.

[12] G. Biener, A. Niv, V. Kleiner, and E. Hasman, "Metallic subwavelength structures for a broadband infrared absorption control," *Opt. Lett.,* vol. 32, pp. 994-996, 2007.

[13] M. D. Groner, F. H. Fabreguette, J. W. Elam, and S. M. George, "Low-temperature Al_2O_3 atomic layer deposition," *Chem. Mater.,* vol. 16, pp. 639-645, 2004.

[14] T. Aaltonen, M. Ritala, T. Sajavaara, J. Keinonen, and M. Leskelä, "Atomic layer deposition of platinum thin films," *Chem. Mater.*, vol. 15, pp. 1924-1928, 2003.

[15] K. R. Williams, K. Gupta, and M. Wasilik, "Etch rates for micromachining processing-part II," *J. Microelectromech. Syst.,* vol. 12, pp. 761-778, 2003.

[16] J. Vancea, H. Hoffmann, and K. Kastner, "Mean free path and effective density of conduction electrons in polycrystalline metal films," *Thin Solid Films,* vol. 121, pp. 201-216, 1984.